frontiers in Physiology

ORIGINAL RESEARCH
published: 29 May 2017
doi: 10.3389/fphys.2017.00342

Icariin, a Novel Blocker of Sodium and Calcium Channels, Eliminates Early and Delayed Afterdepolarizations, As Well As Triggered Activity, in Rabbit Cardiomyocytes

*Wanzhen Jiang †, Mengliu Zeng †, Zhenzhen Cao, Zhipei Liu, Jie Hao, Peipei Zhang, Youjia Tian, Peihua Zhang and Jihua Ma **

Cardio-Electrophysiological Research Laboratory, Medical College, Wuhan University of Science and Technology, Hubei, China

OPEN ACCESS

Edited by:
Zhilin Qu,
University of California, Los Angeles, United States

Reviewed by:
Milan Stengl,
Charles University in Prague, Czechia
Edward Joseph Vigmond,
University of Bordeaux 1, France

***Correspondence:**
Jihua Ma
mjhua@wust.edu.cn

† These authors have contributed equally to this work.

Specialty section:
This article was submitted to Cardiac Electrophysiology, a section of the journal Frontiers in Physiology

Received: *22 February 2017*
Accepted: *09 May 2017*
Published: *29 May 2017*

Citation:
Jiang W, Zeng M, Cao Z, Liu Z, Hao J, Zhang P, Tian Y, Zhang P and Ma J (2017) Icariin, a Novel Blocker of Sodium and Calcium Channels, Eliminates Early and Delayed Afterdepolarizations, As Well As Triggered Activity, in Rabbit Cardiomyocytes. Front. Physiol. 8:342. doi: 10.3389/fphys.2017.00342

Icariin, a flavonoid monomer from *Herba Epimedii*, has confirmed pharmacological and biological effects. However, its effects on arrhythmias and cardiac electrophysiology remain unclear. Here we investigate the effects of icariin on ion currents and action potentials (APs) in the rabbit myocardium. Furthermore, the effects of icariin on aconitine-induced arrhythmias were assessed in whole rabbits. Ion currents and APs were recorded in voltage-clamp and current-clamp mode in rabbit left ventricular myocytes (LVMs) and left atrial myocytes (LAMs), respectively. Icariin significantly shortened action potential durations (APDs) at 50 and 90% repolarization (APD_{50} and APD_{90}) and reduced AP amplitude (APA) and the maximum upstroke velocity (V_{max}) of APs in LAMs and LVMs; however, icariin had no effect on resting membrane potential (RMP) in these cells. Icariin decreased the rate-dependence of the APD and completely abolished anemonia toxin II (ATX-II)-induced early afterdepolarizations (EADs). Moreover, icariin significantly suppressed delayed afterdepolarizations (DADs) and triggered activities (TAs) elicited by isoproterenol (ISO, 1 μM) and high extracellular calcium concentrations ($[Ca^{2+}]_o$, 3.6 mM) in LVMs. Icariin also decreased I_{NaT} in a concentration-dependent manner in LAMs and LVMs, with IC_{50} values of 12.28 ± 0.29 μM (n = 8 cells/4 rabbits) and 11.83 ± 0.92 μM (n = 10 cells/6 rabbits; $p > 0.05$ vs. LAMs), respectively, and reversed ATX-II-induced I_{NaL} in a concentration-dependent manner in LVMs. Furthermore, icariin attenuated I_{CaL} in a dose-dependent manner in LVMs. The corresponding IC_{50} value was 4.78 ± 0.89 μM (n = 8 cells/4 rabbits), indicating that the aforementioned current in LVMs was 2.8-fold more sensitive to icariin than I_{CaL} in LAMs (13.43 ± 2.73 μM; n = 9 cells/5 rabbits). Icariin induced leftward shifts in the steady-state inactivation curves of I_{NaT} and I_{CaL} in LAMs and LVMs but did not have a significant effect on their activation processes. Moreover, icariin had no effects on I_{K1} and I_{Kr} in LVMs or I_{to} and I_{Kur} in LAMs. These

results revealed for the first time that icariin is a multichannel blocker that affects I_{NaT}, I_{NaL} and I_{CaL} in the myocardium and that the drug had significant inhibitory effects on aconitine-induced arrhythmias in whole rabbits. Therefore, icariin has potential as a class I and IV antiarrhythmic drug.

Keywords: icariin, antiarrhythmic drug, ion currents, action potential, cardiomyocytes

INTRODUCTION

Icariin ($C_{33}H_{40}O_{15}$, molecular weight = 676.7), the chemical structure of which has been reported by Tao et al. (2013), is a flavonoid monomer extracted from *Herba Epimedii*. It has been confirmed to have a variety of pharmacological and biological effects, including anti-inflammatory (Xu et al., 2010; Tao et al., 2013), antioxidant (Liu et al., 2004; Huang et al., 2014), anti-tumor (Wang et al., 2011; Tan et al., 2016), and neuroprotective effects (Liu et al., 2011). It was recently reported that icariin protected H9c2 cells from apoptosis by inhibiting endoplasmic reticular stress and the reactive oxygen species-dependent JNK and p38 pathways (Zhang et al., 2013; Zhou et al., 2014). Icariin was also found to ameliorate cardiac remodeling and left ventricular dysfunction in rats with heart failure by attenuating matrix metalloproteinase activity and myocardial apoptosis (Song et al., 2011). Furthermore, icariin protected the heart from ischemia-reperfusion injury through PI3K-Akt signaling pathway activation (Ke et al., 2015). Additionally, Sun et al. (2011) found that icariin facilitated the differentiation of mouse embryonic cells into cardiomyocytes. The results of these studies indicate that icariin has cardioprotective effects. However, the effects of icariin on APs and ion channels in cardiomyocytes have not been reported. Thus, the aim of the present study was to investigate the effects of icariin on action potentials (APs), ion currents in cardiomyocytes, as well as arrhythmias in whole rabbits, and to further investigate the medicinal value of icariin for the treatment of heart diseases.

MATERIALS AND METHODS

Cardiomyocyte Isolation

The animal experiments performed in this investigation conformed to the Guide for Care and Use of Laboratory Animals of Hubei Province, China, and the study protocol was approved by Experimental Animal Ethics Committee of Wuhan University of Science and Technology. Hearts from adult New Zealand white rabbits (1.5–2 kg) of either sex were quickly removed and retrogradely perfused by the Langendorff method, as described previously (Wu, 2005), with Ca^{2+}-free Tyrode solution containing the following compounds (in mM): 135 NaCl, 5.4 KCl, 1.0 $MgCl_2$, 10 glucose, 0.33 NaH_2PO_4, and 10 HEPES, pH 7.4 with NaOH for 5 min. Then, hearts were perfused with Ca^{2+}-free Tyrode solution containing collagenase type I (1 g/l) and bovine serum albumin (BSA, 1 g/l) for 30–40 min before being perfused with KB solution for another 5 min. After perfusion, the left ventricle and left atrium were isolated and gently agitated in KB solution. The cardiomyocytes were filtered through a nylon mesh and stored in KB solution containing the following compounds (in mM): 70 KOH, 40 KCl, 20 KH_2PO4, 50 glutamic acid, 20 taurine, 0.5 EGTA, 10 glucose, 10 HEPES, and 3.0 MgSO4, pH 7.4 with KOH. All solutions used in this study were saturated with 95% O_2 and 5% CO_2 and were maintained at 37°C.

AP Recordings

For AP recording, quiescent and Ca^{2+}-tolerant cardiomyocytes were bathed in standard Tyrode solution. The patch pipette solution contained the following reagents (in mM): 110 K-aspartate, 30 KCl, 5 NaCl, 10 HEPES, 0.1 EGTA, 5 MgATP, 5.0 creatine phosphate, and 0.05 CAMP, pH 7.2 with KOH. When filled with pipette solution, the electrode resistance was in the range of 1.5–2.5 MΩ. APs were induced in current-clamp mode by 1.5-fold diastolic threshold current pulses of 5 ms in duration at different pacing cycle lengths (CLs).

Ion Current Recordings

Currents were recorded with a patch-clamp amplifier (EPC9, Heka electronic, Lambrecht, Pfalz, Germany) and were filtered at 2 kHz and digitized at 10 kHz.

The bath solution used for I_{NaT} recording contained the following compounds (in mM): 30 NaCl, 1.0 $CaCl_2$, 105 CsCl, 1.0 $MgCl_2$, 0.05 CdCl, 5.0 HEPES, and 5.0 glucose, pH 7.4 with CsOH, and 1 μM nicardipine was added to the bath solution to block I_{CaL}. The pipette solution contained the following compounds (in mM): 120 CsCl, 1.0 $CaCl_2$, 5.0 $MgCl_2$, 5.0 Na_2ATP, 10 TEA-Cl, 11 EGTA, and 10 HEPES, pH 7.3 with CsOH. I_{NaT} was determined by 300-ms depolarization pulses from −70 mV to +40 mV in 5-mV increments—using a holding potential (HP) of −90 mV—at 0.5 Hz. For the steady-state inactivation protocols, currents were recorded using 100-ms conditional prepulses from −100 mV to −50 mV in 5 mV increments—using a HP of −90 mV—followed by a 100-ms test pulse at −20 mV and 0.5 Hz.

The bath solution used for I_{NaL} recording contained the following compounds (in mM): 135 NaCl, 5.4 CsCl, 1.0 $MgCl_2$, 10 glucose, 0.33 NaH_2PO_4, 0.3 $BaCl_2$, 10 HEPES, and 1.8 $CaCl_2$,

Abbreviations: AP, action potential; LAM, left atrial myocyte; LVM, left ventricular myocyte; APD, action potential duration; APD_{50} and APD_{90}, APD at 50 and 90% repolarization; V_{max}, maximum upstroke velocity of AP; APA, AP amplitude; RMP, resting membrane potential; RD, rate dependence of the APD; RRD, reverse rate dependence of the APD; ATX-II, anemonia toxin II; EAD, early afterdepolarization; DAD, delayed afterdepolarization; TA, triggered activity; ISO, isoproterenol; $[Ca^{2+}]_o$, extracellular calcium concentration; I_{NaT}, transient sodium current; I_{CaL}, L-type calcium current; I_{NaL}, late sodium current; I_{K1}, inward rectifier potassium current; I_{Kr}, rapid component of delayed rectifier potassium current; I_{to}, transient outward potassium current; I_{Kur}, ultra-rapid delayed rectifier potassium current; CL, cycle length; ventricular premature contraction (VPC); ventricular tachycardia (VT); ventricular fibrillation (VF).

pH 7.4 with NaOH, and 1 μM nicardipine was added to the bath solution to block I_{CaL}. The pipette solution used for this experiment was the same as that used for I_{NaT} recording I_{NaL} was recorded using a 300-ms depolarization pulse at a HP of −90 mV, followed by pulses with potentials that were increased from −80 mV to +60 mV in 10-mV increments, and was measured at 200 ms in depolarization testing pulse.

The bath solution (except nicardipine) used for I_{CaL} recording was the same as that used for I_{NaL} recording. The electrode was filled with an internal solution containing the following compounds (in mM): 80 CsCl, 60 CsOH, 40 aspartate acid, 0.65 $CaCl_2$,5.0 HEPES, 10 EGTA, 5.0 MgATP, and 5.0 Na_2-creatine phosphate, pH 7.2 with CsOH. I_{CaL} was determined using 300-ms voltage steps with potentials that were increased from −40 mV to +50 mV in 5-mV increments at 0.5 Hz. For the steady-state inactivation protocol, I_{CaL} was determined using 2,000-ms conditional prepulses with potentials that were increased from −50 mV to 0 mV in 5-mV increments—using a HP of −40 mV—followed by a 300-ms test pulse at 0 mV.

For I_{K1} recording, the cells were bathed with Tyrode solution, and 1 μM nicardipine was used to block I_{CaL}. The internal solution contained the following compounds (in mM): 140 KCl, 1.0 $MgCl_2$, 5.0 K_2ATP, 10 EGTA, and 5.0 HEPES, pH 7.3 with KOH.

The external solution used to record I_{Kr} contained the following compounds (in mM): 135 NaCl5.4 KCl, 1.0 $MgCl_2$, 5.0 glucose, 0.2 $CdCl_2$, 0.33 NaH_2PO_4, 5.0 HEPES, and 1.0 $CaCl_2$, pH 7.4 with NaOH, and 30 μM chromanol 293B was used to block I_{Ks}. The pipette solution contained the following compounds (in mM): 140 KCl, 1.0 $MgCl_2$, 2.0 Na_2ATP, 10 EGTA, and 5.0 HEPES, pH 7.25 with KOH.

The bath solution used to elicit I_{to} contained the following compounds (in mM): 140 NaCl, 5.4 KCl, 1.0 $MgCl_2$, 10 glucose, 0.33 NaH_2PO_4, 5 HEPES, and 1.8 $CaCl_2$, pH 7.4 with NaOH. The internal solution contained the following compounds (in mM): 110 K-aspartate, 20 KCl, 0.1 GTP, 1.0 $MgCl_2$, 10 HEPES, 5.0 EGTA, 5.0 MgATP, and 5.0 creatine phosphate, pH 7.2 with KOH. $BaCl_2$(200 μM), $CdCl_2$ (200 μM), and atropine (1 μM) were used to block I_{K1}, I_{CaL}, and I_{KAch}, respectively.

The bath solution and pipette solution used to record I_{Kur} were the same as those used to record I_{to}, but the pulse protocol was different from that used to record I_{to} (see the Results Section).

Aconitine-Induced Arrhythmias in Whole Rabbits

Twenty healthy New Zealand rabbits were randomly divided into two groups ($n = 10$ for each group): normal saline (NS) and icariin. In the NS group, saline was injected intraperitoneally within half an hour before the experiment. In the icariin group, 3 mg/kg icariin was injected intraperitoneally within half an hour before the experiment. At the beginning of the experiments, both groups of rabbits were anesthetized with xylazine (7.5 mg/kg, i.m.) and ketamine (30 mg/kg, i.v.) through ear vein injection. A standard limb lead II electrocardiogram (ECG) was recorded using the BL-420F data acquisition and analysis system (Chengdu TaiMeng, Sichuan, China) for 120 min following the application of 2 μg/kg/min aconitine, which was injected by a constant velocity pump and used to induce arrhythmias. The onset time and onset dosage of aconitine that induced ventricular premature contraction (VPC), ventricular tachycardia (VT) and ventricular fibrillation (VF) were measured.

Drugs and Reagents

Icariin (purity >97%) was obtained from Sigma Aldrich (Saint Louis, MO, USA). Collagenase type I and CsCl were purchased from Gibco (GIBCO TM, Invitrogen Co., Paisley, UK). BSA and HEPES were obtained from Roche (Basel, Switzerland), and the other chemicals were obtained from Sigma Aldrich (Saint Louis, MO, USA). Dimethyl sulfoxide (DMSO) was used to dissolve icariin to obtain a 1 mM stock solution. The final concentration of the DMSO added to the bath solution was less than 0.1%.

Data Analysis

Fitmaster (v2x32, HEKA) was used for data analysis, and the figures were plotted by Origin 8.0 (OriginLab Co., MA, USA). All data were expressed as the mean ± SD. Data pertaining to the I_{NaT} and I_{CaL} steady-state activation and steady-state inactivation relationships were fitted by the Boltzmann equation, $Y = 1/\{1+\exp\ (V_m - V_{1/2})/k\}$, where V_m is the membrane potential, $V_{1/2}$ is the half-activation and half-inactivation potential, k is the slope factor, and Y is relative conductance (G/G_{max}, steady-state activation) and relative current (I/I_{max}, steady-state inactivation). The dose-response relationship curves for the effects of icariin on I_{NaT} and I_{CaL} were fitted to the Hill equation, $(I_{control} - I_{drug})/I_{drug} = E_{max}/[1 + (IC_{50}/C)^n]$, where $I_{control}$ and I_{drug} represent the amplitude of I_{NaT} and I_{CaL} obtained in the absence and presence of icariin, respectively, E_{max} is the maximum inhibition, IC_{50} is the concentration of icariin at which its half-maximum inhibitory effects are exerted, C is the concentration of icariin, and n is the Hill coefficient. Current density was calculated by dividing the current amplitude by the cell capacitance. The statistical significance of the differences between two groups was determined by Student's t-test, and mean comparisons among multiple groups were performed by one-way analysis of variance (ANOVA) followed by Bonferroni's test. $P < 0.05$ was considered significant.

RESULTS

Figure 1A shows the representative morphologies of a single isolated left ventricular myocyte (LVM, left) and left atrial myocyte (LAM, right). The rod-shaped LVM had glossy and smooth edges, as well as the typical transverse striations. The LAM was more slender than the LVM.

Effects of Icariin on Action Potentials

APs were consecutively recorded by 5-ms and 1.5-fold threshold current pulses at 1 Hz in the absence and presence of icariin. Icariin attenuated AP amplitude (APA) and the maximum upstroke velocity (V_{max}), shortened action potential durations (APDs) at 50 and 90% repolarization (APD_{50} and APD_{90}, respectively) in a concentration-dependent manner in LVMs and

LAMs. However, icariin had no significant effects on resting membrane potential (RMP) at concentrations of 5 and 10 μM (**Figure 1B**; **Table 1**).

In our study, 5 and 10 μM icariin attenuated the rate-dependence (RD) of the APDs (n = 9 cells/4 rabbits; **Figures 1C,D**) in LVMs by 10.5 ± 4.3% and 28.5 ± 7.2% at a pacing cycle length (CL) of 500 ms, by 13 ± 4.9% and 32.2 ± 7.4% at a pacing CL of 1,000 ms and by 16.5 ± 4.8% and 34.5 ± 6.4% at a pacing CL of 2,000 ms, respectively.

Effects of Icariin on Cellular Arrhythmias

In the present study, we used 10 nM anemonia toxin II (ATX-II) and a stimulation frequency of 0.25 Hz to elicit early afterdepolarizations (EADs) in LVMs. ATX-II significantly lengthened the APD from 179.78 ± 18.64 ms to 1186.44 ± 93.13 ms and induced EADs in 7 of 10 cells (70%; n = 10 cells/5 rabbits; **Figures 2A–C**), and 20 μM icariin decreased the APs prolonged by ATX-II from 1186.44 ± 93.13 ms to 360.08 ± 41.95 ms and completely abolished the EADs induced by ATX-II in seven cells. In another group, to elicit delayed afterdepolarizations (DADs) and triggered activities (TAs) in LVMs, we added 1 μM isoproterenol (ISO) to the external solution and the extracellular calcium concentration was elevated to 3.6 mM following a baseline pacing CL of 9,000 ms and on top of that 15 beats with a stimulation frequency of 2.5 Hz. DADs were noted in 6 of 9 cells (3 rabbits; 66.7%), and TAs were noted in 3 of 9 cells (33.3%). Administration of 10 μM icariin significantly suppressed the ISO-induced DADs and completely abolished the ISO-induced TAs (**Figure 2D**).

Effects of Icariin on I_{NaT} and I_{NaL}

When the effects of icariin on I_{NaT} reached a steady state (3 min), the next concentration of the drug could be added to the external recording solution. Icariin (1, 5, 10, and 20 μM) reduced I_{NaT} in a dose-dependent manner in LVMs and LAMs. **Figures 3A,B** show the representative recordings for I_{NaT} in LVMs and LAMs,

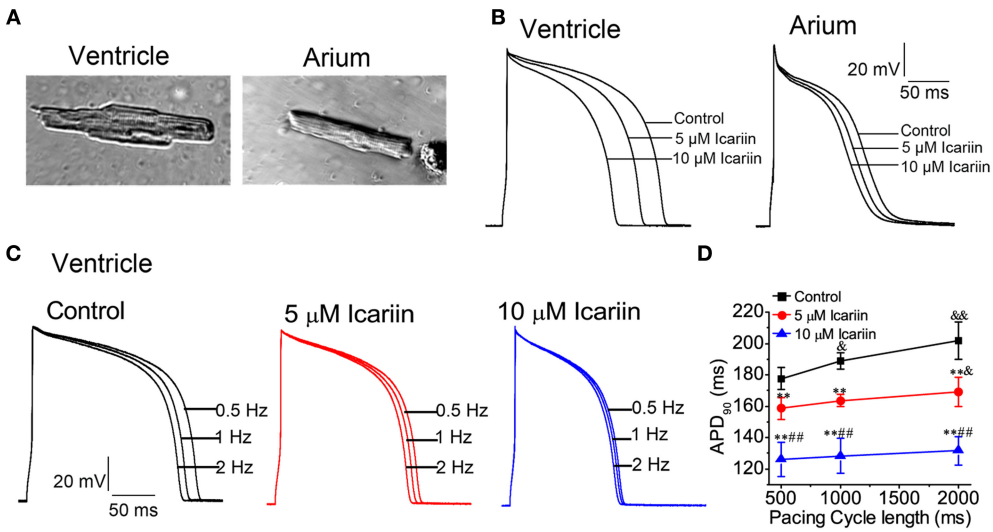

FIGURE 1 | Icariin attenuated APDs in a concentration- and rate-dependent manner in rabbit LVMs and LAMs. (A). Photomicrograph of a single LVM (left) and LAM (right). **(B)**. Effects of icariin (5 and 10 μM) on APs elicited at a stimulation frequency of 1 Hz in LVMs (left) and LAMs (right). **(C)**. Representative recordings of APs elicited at 0.5 Hz, 1 Hz and 2 Hz in the absence and presence of icariin (5 and 10 μM) in ventricular myocytes. **(D)**. Data pertaining to APD_{90} from 30 sequential curves were averaged. The averaged data for different pacing CLs are shown, n = 9 cells/4 rabbits. $^{\&}$ and $^{\&\&}p < 0.05$ and 0.01 vs. a pacing CL of 500 ms; $^{**}p < 0.01$ vs. control at the same pacing CL; $^{\#\#}p < 0.01$ vs. 5 μM icariin at the same pacing CL.

TABLE 1 | Effects of icariin on action potentials (APs) in rabbit LVMs and LAMs.

	Ventricle (n = 14 cells/7 rabbits)			Atrium (n = 14 cells/6 rabbits)		
Parameters	**Control**	**5 μM icariin**	**10 μM icariin**	**Control**	**5 μM icariin**	**10 μM icariin**
RMP(mV)	−81 ± 2	−81 ± 3	−81 ± 5	−77 ± 3	−77 ± 4	−77 ± 6
APA(mV)	114 ± 5	111 ± 6	108 ± 9*	107 ± 7	104 ± 6	100 ± 5*
V_{max}(V/s)	168 ± 10	146 ± 8*	131 ± 6*†	231 ± 10	222 ± 7	205 ± 13*†
APD_{50}(ms)	158 ± 6	127 ± 5*	107 ± 3*†	103 ± 4	90 ± 9*	72 ± 7*†
APD_{90}(ms)	188 ± 4	157 ± 3*	131 ± 4*†	135 ± 8	122 ± 12*	104 ± 11*†

*RP, resting membrane potential; APA, action potential amplitude; V_{max}, maximum upstroke velocity; APD_{50}, action potential duration at 50% repolarization; APD_{90}, action potential duration at 90% repolarization. *$p < 0.05$ vs. control; †$p < 0.05$ vs. 5 μM icariin.*

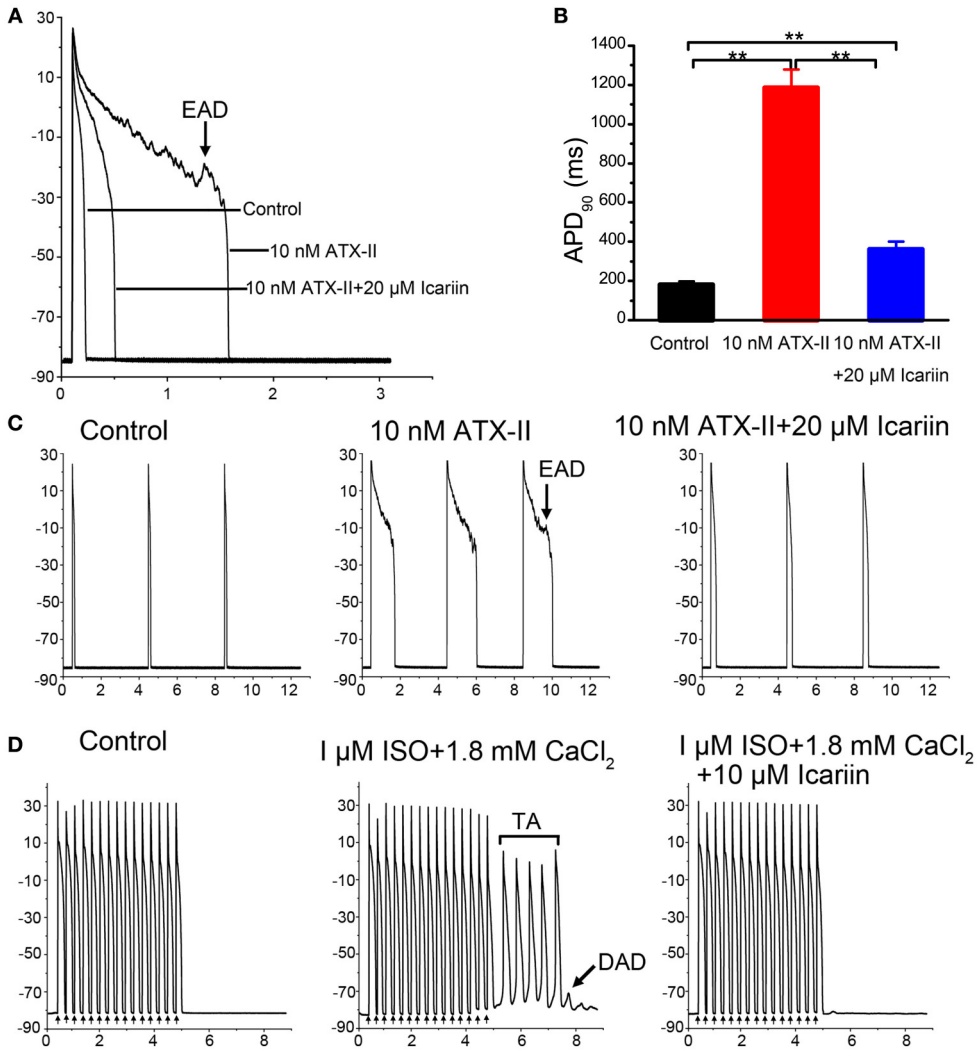

FIGURE 2 | Effects of icariin on EADs and DADs, as well as TAs, in LVMs. (A,C). Administration of 20 μM Icariin completely abolished the EADs and attenuated the AP prolongations induced by 10 nM ATX-II at a stimulation frequency of 0.25 Hz. Single beats or 3 consecutive beats are displayed in **(A,C)**, respectively. **(B)** Summary data for APD_{90} after sequential administration of 10 nM ATX-II and 20 μM icariin. $^{**}p < 0.01$. **(D)**. DADs and TAs were induced in LVMs by a baseline pacing CL of 9,000 ms and on top of that 15 beats with a stimulation frequency of 2.5 Hz after superfusion with ISO (1 μM) and a high extracellular calcium concentration ($[Ca^{2+}]_o$, 3.6 mM). Administration of 10 μM icariin significantly suppressed the DADs and completely abolished the TAs induced by ISO and calcium.

respectively, and **Figure 3C** shows the corresponding current-voltage relationships in LVMs and LAMs. The IC_{50} values for I_{NaT} in LVMs and LAMs were 11.83 ± 0.92 μM (n = 10 cells/6 rabbits) and 12.28 ± 0.29 μM (n = 8 cells/4 rabbits; $p > 0.05$ LAMs vs. LVMs; **Figure 3D**), respectively. **Figures 3E,G** show typical current recordings, which were generated according to the steady-state inactivation protocol, in LVMs and LAMs. In the absence and presence of 20 μM icariin, the $V_{1/2}$ values of the steady-state inactivation curves in LVMs were −85.47 ± 1.36 mV and −91.45 ± 1.48 mV (n = 8 cells/5 rabbits; $p < 0.01$ vs. control), respectively, with corresponding k-values of 8.48 ± 1.05 and 8.28 ± 0.76 (n = 8 cells/5 rabbits; $p > 0.05$ vs. control). Administration of 20 μM icariin shifted the $V_{1/2}$ value of the steady-state inactivation curve in LAMs from −76.1 ± 1.52 mV to −82.28 ± 0.96 mV (n = 6 cells/3 rabbits; $p < 0.01$ vs. control), with k-values of 8.29 ± 1.64 and 8.72 ± 0.81 (n = 6 cells/3 rabbits; $p > 0.05$ vs. control). These results indicate that icariin induced a leftward (negative potential) shift of the steady-state inactivation curve of I_{NaT} in LVMs and LAMs (**Figures 3F,H**). However, it had no significant effects on the activation process in LVMs and LAMs (**Figures 3F,H**).

To identify I_{NaL}, we recorded current before and after the application of 4 μM TTX using 300-ms depolarization pulses with potentials ranging from a HP of −90 mV to a potential of −20 mV. TTX (4 μM) had no significant effects on I_{NaT} but decreased the amplitude of I_{NaL} from −0.39 ± 0.004 pA/pF to 0.023 pA/pF (n = 6 cells/3 rabbits; $p < 0.01$ vs. control), indicating that the TTX-sensitive current was I_{NaL}.

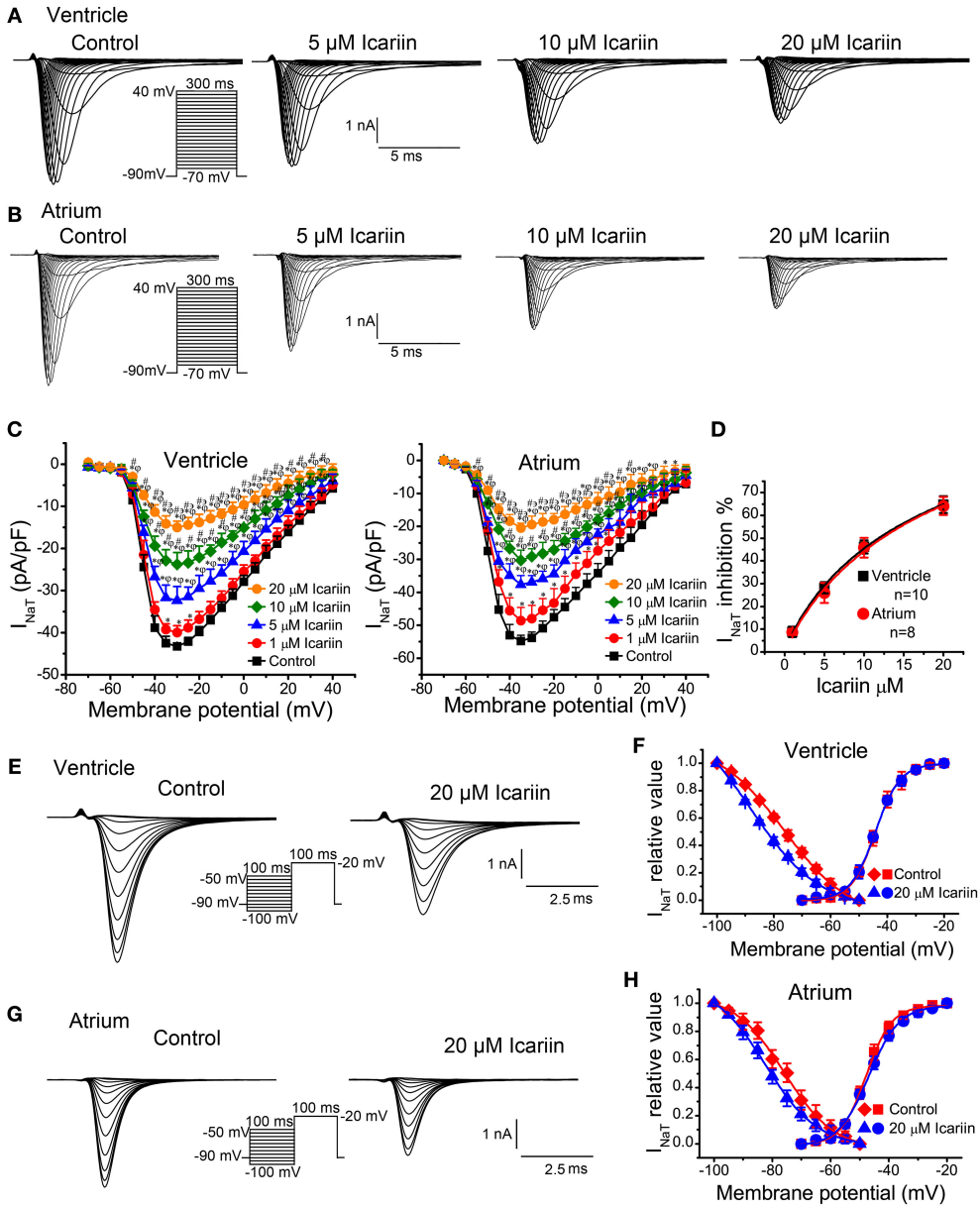

FIGURE 3 | Effects of icariin on I_{NaT} in LVMs and LAMs. (A,B). Representative recordings of I_{NaT} in LVMs **(A)** and LAMs **(B)** after sequential applications of 5, 10, and 20 μM icariin. **(C)**. Current-voltage relationship of I_{NaT} in LVMs (left; $n = 10$ cells/6 rabbits) and LAMs (right; $n = 13$ cells/5 rabbits) in the absence and presence of icariin. $^{*}p < 0.05$ vs. control; $^{\varphi}p < 0.05$ vs. 1 μM icariin; $^{\#}p < 0.05$ vs. 5 μM icariin; $^{\ni}p < 0.05$ vs. 10 μM icariin. **(D)**. The dose-response relationships illustrating icariin-induced decreases in I_{NaT} in LVMs and LAMs. Data were fitted by the Hill equation. **(E,G)**. Representative current recordings of I_{NaT} elicited according to the steady-state inactivation protocol in LVMs **(E)** and LAMs **(G)** in the absence and presence of 20 μM icariin. (**(F)**. Steady-state activation ($n = 8$ cells/4 rabbits) and steady-state inactivation ($n = 8$ cells/5 rabbits) curves of I_{NaT} in LVMs before and after icariin administration. (**(H)**. Steady-state activation ($n = 8$ cells/4 rabbits) and steady-state inactivation ($n = 6$ cells/3 rabbits) curves of I_{NaT} in LAMs before and after icariin administration.

Administration of 10 nM ATX-II significantly enhanced I_{NaL}, an effect that was reversed by administration of 1, 10, 20, and 40 μM icariin ($n = 6$ cells/4 rabbits; **Figures 4A,C**). The percentage inhibitions by 1, 10, 20, and 40 μM icariin of ATX-II augmented I_{NaL} were 7.8 ± 1%, 29 ± 6.4%, 43.68 ± 5.6%, and 61.4 ± 5.7%. **Figure 4B** shows the representative current recordings of I_{NaL} at −20 mV that are shown in **Figure 4A**.

Effects of Icariin on I_{CaL}

To elicit I_{CaL}, we clamped LVMs at −40 mV and then depolarized the cells to +5 mV for 300 ms at 0.2 Hz. As shown in **Figure 5A**, the I_{CaL} run-down phenomenon lasted for approximately 5 min after membrane rupture in the control condition and then reached a steady state for 15 min ($n = 5$ cells/2 rabbits). I_{CaL} decreased by 8.5% during the this 5-min period. We performed

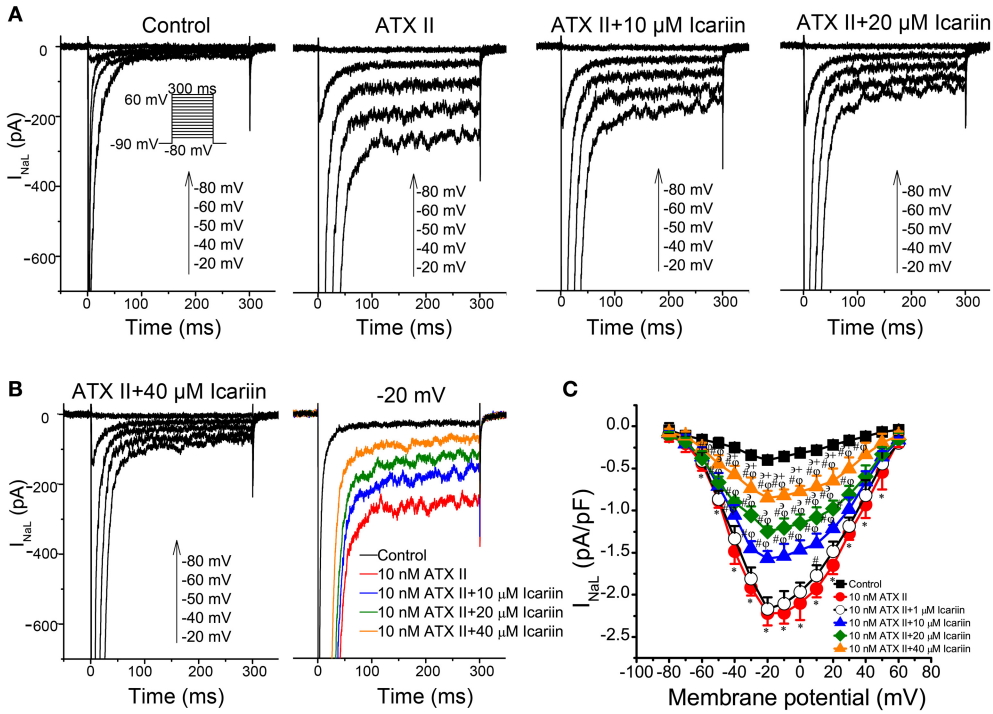

FIGURE 4 | Effects of icariin on ATX-II-induced increases in I_{NaL} in LVMs. (A). Representative current recordings of I_{NaL} in LVMs after sequential treatments with 10 nM ATX-II and 10, 20, and 40 μM icariin. (**B**). Representative current recordings of I_{NaL} at −20 mV from **(A,C)**. The current-voltage relationship of I_{NaL} in LVMs, $n = 6$ cells/4 rabbits. $^{*}p < 0.05$ vs. control; $^{\#}p < 0.05$ vs. 10 nM ATX-II; $^{\varphi}p < 0.05$ vs. 1 μM icariin; $^{\ni}p < 0.05$ vs. 10 μM icariin; $^{+}p < 0.05$ vs. 20 μM icariin.

a series of experiments on I_{CaL} during the stabilization period. To investigate the efficiency of the effects of icariin on I_{CaL} in LVMs, we recorded the current sequentially. As shown in **Figure 5B**, 10 μM icariin was added to the bath solution after the first (1st) current curve (control). I_{CaL} decreased rapidly between the tenth (10th) current curve (45 s after perfusion with icariin) and the thirteenth (13th) current curve (60 s after perfusion with icariin) and then decreased gradually until it reached a steady state (the twenty-seventh current curve). Icariin was washed out after 27th current curve (130 s after perfusion with icariin). I_{CaL} increased rapidly between the 27th current curve and the thirtieth (30th) current curve and then increased gradually until it reached its maximum value (82%) at the fifty-fifth current curve (270 s after perfusion with icariin). The summary data are shown in **Figure 5C** ($n = 10$ cells/4 rabbits). The above results indicate that icariin rapidly and reversibly inhibited I_{CaL} in LVMs.

When the effects of icariin on I_{CaL} reached a steady state (2.5 min), the next concentration of the drug could be added to the bath solution. **Figure 5D** shows the representative I_{CaL} recordings in LVMs after sequential treatments of 0.1, 1, 5, 10 μM icariin and 1 μM nicardipine. Icariin decreased I_{CaL} in a concentration-dependent manner in LVMs, with an IC_{50} of 4.78 ± 0.89 μM ($n = 8$ cells/4 rabbits; **Figure 5G**). Nicardipine (1 μM) almost completely inhibited I_{CaL} in LVMs in the presence of 10 μM icariin, indicating that I_{CaL} was the nicardipine-sensitive current. **Figure 5E** shows the representative I_{CaL} recordings in LAMs after sequential treatments of 1, 5, 10, and 20 μM icariin. Icariin reduced I_{CaL} in a dose-dependent manner in LAMs, with an IC_{50} of 13.43 ± 2.73 μM ($n = 9$ cells/5 rabbits; $p < 0.01$ vs. LVMs; **Figure 5G**). **Figure 5F** shows the I_{CaL} current-voltage relationships in LVMs (left, $n = 13$ cells/6 rabbits) and LAMs (right, $n = 9$ cells/5 rabbits). Icariin shifted the I_{CaL} steady-state inactivation curves to the left in LVMs and LAMs (**Figures 5I,K**). The $V_{1/2}$ values before and after 10 μM icariin administration were shifted from −25.7 ± 1.01 mV and −29.96 ± 0.85 mV to −28.87 ± 2.18 mV ($n = 10$ cells/4 rabbits; $p < 0.01$ vs. control; **Figures 5H,I**) and −33.94 ± 1.33 mV ($n = 10$ cells/6 rabbits; $p < 0.01$ vs. control; **Figures 5J,K**), and the k-values were shifted from 7.16 ± 1.08 and 5.86 ± 0.82 to 7.52 ± 2.31 ($p > 0.05$ vs. control) and 7.4 ± 1.14 ($p < 0.01$ vs. control) in LVMs and LAMs, respectively. However, the drug has no significant effects on the activation process in these cells (**Figures 5I,K**).

Effects of Icariin on Main Potassium Currents

To elicit I_{K1} in LVMs, we clamped the cells at −40 mV (to inactivate their sodium channels) and depolarized them from −120 mV to +50 mV in 5-mV increments for 400 ms at 0.5 Hz. As shown in **Figures 6A,B**, icariin (10 and 40 μM) had no effect on I_{K1} ($n = 18$ cells/8 rabbits). I_{Kr} in LVMs was elicited using a 3-s depolarization pulse whose potential was increased from a HP of −40 mV to a potential of 50 mV in 10-mV increments before returning to a potential of −40 mV for 5 s. Only the I_{Kr} tail-current ($I_{Kr-tail}$) was measured. Icariin (10 and 40 μM)

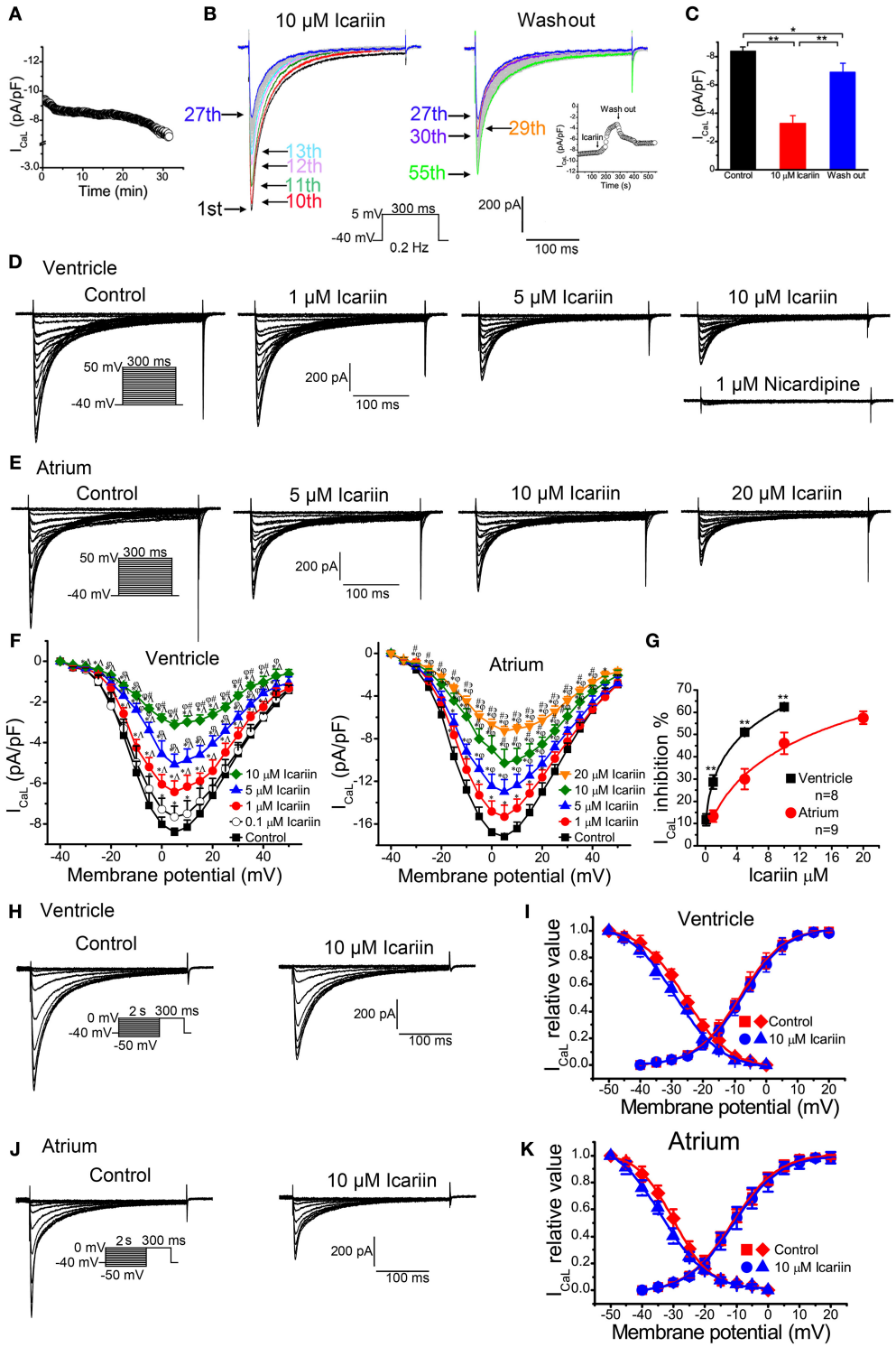

FIGURE 5 | Effects of icariin on I_{CaL} in LVMs and LAMs. (A). Time course of the I_{CaL} run-down phenomenon in LVMs under the control condition, $n = 5$ cells/2 rabbits. I_{CaL} were evoked by 300-ms depolarization pulses ranging from a holding potential of −40 mV to 5 mV at 0.2 Hz. **(B)**. Consecutive recordings of I_{CaL} evoked by a 300-ms depolarization from a holding potential of −40 mV to 5 mV at 0.2 Hz. The 1st sweep represents the control condition, the 2nd to 27th sweeps represent the period in which icariin exerted its effects on I_{CaL}, and the 27th–55th sweeps indicate the period in which the effects of icariin on I_{CaL} were reversed. The inset represents the time course of the entire process, including the control condition, the icariin perfusion period, and the icariin

(Continued)

FIGURE 5 | Continued
wash-out period. The entire process was conducted during the stabilization period. (**(C)**. Summary data for the mean current densities of I_{CaL} in the control condition, the icariin perfusion period, and the icariin wash-out period, $n = 10$ cells/4 rabbits. * and ** $p < 0.05$ and 0.01. **(D)**. Representative current recordings of I_{CaL} in LVMs after sequential applications of 1, 5, and 10 μM icariin. **(E)**. Representative current recordings of I_{CaL} in LAMs in the absence and presence of 5, 10, and 20 μM icariin. **(F)**. Current-voltage relationship of I_{CaL} in LVMs (left; $n = 13$ cells/6 rabbits) and LAMs (right; $n = 9$ cells/5 rabbits) before and after the application of icariin. * $p < 0.05$ vs. control; ^ $p < 0.05$ vs. 0.1 μM icariin; $^{\varphi}p < 0.05$ vs. 1 μM icariin; # $p < 0.05$ vs. 5 μM icariin; $^{\ni}p < 0.05$ vs. 10 μM icariin. **(G)**. The dose-response relationships illustrating icariin-induced decreases in I_{CaL} in LVMs and LAMs. * and ** $p < 0.05$ and $p < 0.01$ LVMs vs. LAMs. Data were fitted by the Hill equation. **(H,J)**. Representative current recordings of I_{CaL} evoked according to the steady-state inactivation protocol in LVMs **(H)** and LAMs **(J)** in the absence and presence of 10 μM icariin. **(I)**. Steady-state activation ($n = 14$ cells/7 rabbits) and steady-state inactivation ($n = 10$ cells/4 rabbits) curves of I_{CaL} in LVMs before and after icariin application. **(K)**. Steady-state activation ($n = 12$ cells/7 rabbits) and steady-state inactivation ($n = 10$ cells/6 rabbits) curves of I_{CaL} in LAMs before and after icariin application.

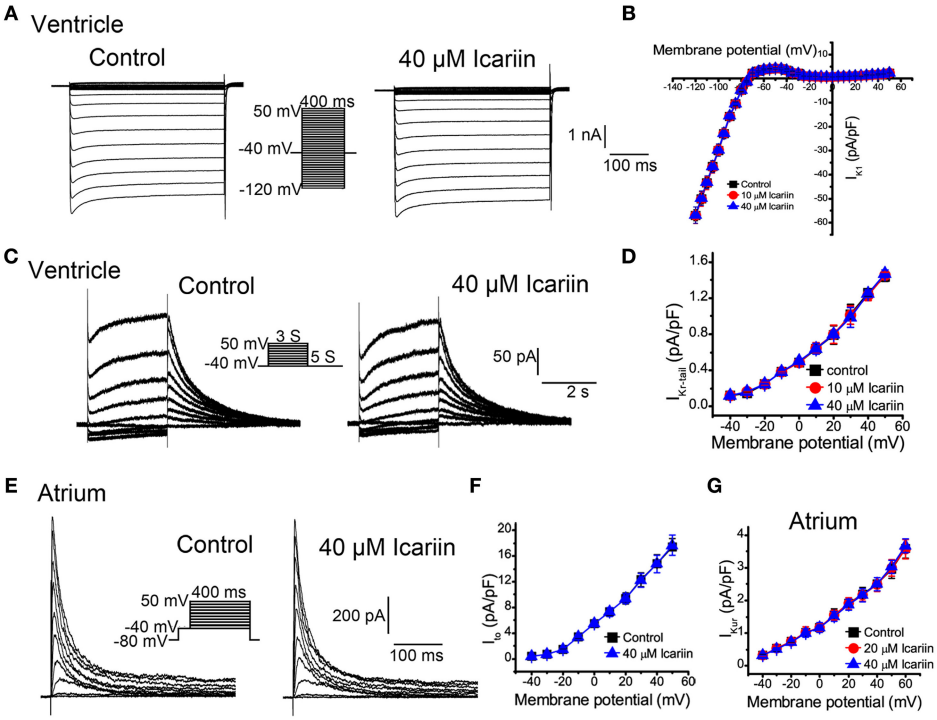

FIGURE 6 | Effects of icariin on the main potassium current in LVMs and LAMs. (A). Representative current recordings of I_{K1} in LVMs before and after 40 μM icariin application. **(B)**. The current-voltage relationship of I_{K1} in LVMs in the absence and presence of icariin, $n = 18$ cells/8 rabbits. **(C)**. Representative current recordings of I_{Kr} in LVMs before and after 40 μM icariin application. **(D)**. The current-voltage relationship of I_{Kr} in LVMs in the absence and presence of icariin, $n = 12$ cells/5 rabbits. **(E)**. Representative current recordings of I_{to} in LAMs before and after 40 μM icariin application. **(F)**. The current-voltage relationship of I_{to} in LAMs in the absence and presence of icariin, $n = 15$ cells/6 rabbits. **(G)**. The current-voltage relationship of I_{Kur} in LAMs before and after icariin application (20 an 40 μM), $n = 15$ cells/5 rabbits.

had no significant effects on $I_{Kr-tail}$ ($n = 12$ cells/5 rabbits; **Figures 6C,D**). I_{to} in LAMs was elicited by 400 depolarization voltage steps with potentials that were increased from −80 mV to +50 mV in 10-mV increments, followed by a conditional test in which −40 mV was administered for 100 ms to block sodium currents. Forty micrometer icariin had no significant effect on I_{to}in LAMs ($n = 15$ cells/6 rabbits; **Figures 6E,F**). I_{Kur} in LAMs was elicited by an 80-ms prepulse whose potential was increased from a HP of −50 mV to a potential of 30 mV (to inactivate I_{to}), followed by 140-ms test pulses with potentials that were increased from −40 mV to +60 mV in 10-mV increments—using a HP of −50 mV—after a 50-ms interval before returning to −30 mV. **Figure 6G** shows the I_{Kur} current-voltage relationship in LAMs in the absence and presence of icariin (20 and 40 μM). Icariin had no significant effect on I_{Kur} ($n = 1$ 5 cells/5 rabbits).

Effects of Icariin on Aconitine-Induced Arrhythmias

In the NS group, VPC, VT, and VF were observed in all 10 rabbits. In the icariin group, VPC, VT and VF occurred in 9, 4 and 1 of 10 rabbits, respectively. Compared with the NS group, icariin application prior to aconitine administration increased the onset time (**Figures 7A,B,D**) and onset dosage (**Figure 7C**). The administration of icariin attenuated the incidence of arrhythmias induced by aconitine (**Figure 7E**) and rabbit mortality (**Figure 7F**).

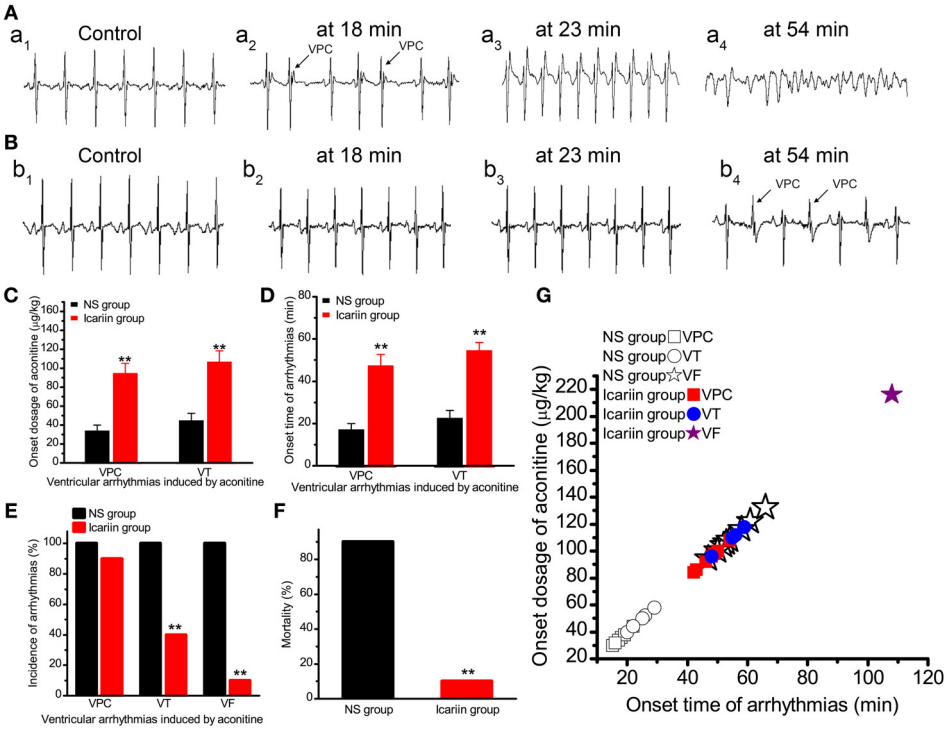

FIGURE 7 | Effects of icariin on aconitine-induced ventricular arrhythmias in whole rabbits. (A). Representative ECG recordings at different onset times of VPC (18 min), VT (23 min) and VF (54 min) in the NS group. **(B)**. Representative ECG recordings consistent with the times of events in **(A)** in the icariin group. **(C,D)**. Histograms show the onset dosage and onset time of aconitine-induced ventricular arrhythmias, respectively. $^{**}p < 0.01$. **(E)**. The incidence of VPC, VT, and VF induced by aconitine in the 2 groups. $^{**}p < 0.01$. **(F)**. Aconitine-induced mortality of rabbits in the 2 groups. $^{**}p < 0.01$. **(G)**. The onset time and onset dosage relationship of the 20 rabbits.

DISCUSSION

The main findings of the present study are as follows: (I) icariin reduced APA and V_{max} of APs, shortened APDs ($APD_{50}$and APD_{90}) in LVMs and LAMs (**Table 1**, **Figure 1B**). (II) Icariin decreased the RD of APD (**Figures 1C,D**) and significantly suppressed EADs and DADs and TAs induced by ATX-II or ISO and high $[Ca^{2+}]_o$, respectively, in LVMs (**Figure 2**). (III) Icariin decreased I_{NaT} in LVMs and LAMs (**Figure 3**) and attenuated the increases in I_{NaL} induced by ATX-II in a concentration dependent manner in LVMs (**Figure 4**). (IV) Icariin blocked I_{CaL} in a dose-dependent manner in LVMs and LAMs (**Figure 5**). Moreover, the inhibitory effects of icariin on I_{CaL} in LVMs were 2.8-fold stronger than those of icariin on the above current in LAMs. (V) Icariin had limited effects on I_{K1} and I_{Kr} in LVMs and on I_{to} and I_{Kur} in LAMs (**Figure 6**). (VI) Icariin inhibited aconitine-induced ventricular arrhythmias (**Figure 7**).

In this study, icariin decreased V_{max} of APs and shortened APDs (APD_{50} and APD_{90}) in a concentration-dependent manner in LVMs and LAMs. The abovementioned decrease in APA and V_{max}, which may be associated with the inhibitory effects of I_{NaT}, can reduce conduction velocities, resulting in reentry blockade (Baba et al., 2005). Moreover, the APD shortening induced by icariin may be closely related to I_{CaL} inhibition because icariin does not affect I_{K1}, I_{Kr}, I_{to}, and I_{Kur}, which also play important roles in maintaining APD. Some drugs displays reverse rate dependence (RRD) of APD property, that is, the effect of a drug to prolong APD may be greater at slow than at fast heart rate, and vice versa. The findings of previous studies suggest that RRD of APD can be induced by enhancing I_{CaL} and inhibiting I_{Kr} or I_{K1}(Bosch et al., 1998; Virag et al., 2009). RRD of APD enhancement leads to an increase in the cardiac transmural dispersion of the repolarization (Osadchii, 2013), which subsequently facilitates the occurrence of reentrant arrhythmias (Coronel et al., 2009; Maoz et al., 2014). In the present study, icariin attenuated I_{CaL} but had no effect on I_{Kr} or I_{K1}, indicating that icariin might diminish or not produce RRD. These results suggest that icariin has increased antiarrhythmic efficiency compared with other drugs and that it is safer than its counterparts.

Sodium channels are known as the key targets of class I antiarrhythmic drugs. I_{NaT} is the main depolarization current in AP phase 0 and plays an important role in myocardial excitability and propagations (Goldin, 2002). In this study, icariin decreased the amplitude of I_{NaT}, which caused a decrease in Na^+ influx. Therefore, the results of this study indicate that icariin can relieve intracellular Na^+ overload and exerts class I antiarrhythmic drug effects.

I_{NaL} is involved in the AP plateau phase (Kiyosue and Arita, 1989). A variety of pathological conditions, such as

ischemia and hypoxia (Saint, 2006), cardiac hypertrophy and heart failure (Valdivia et al., 2005; Guo et al., 2014), can increase I_{NaL}, resulting in an elevated intracellular sodium concentration ($[Na^+]_i$), as well as a subsequent increase in the intracellular Ca^{2+} concentration ($[Ca^{2+}]_i$) as a result of the activity of a reverse Na^+/Ca^{2+} exchanger (NCX), leading to Ca^{2+} overload resulting in arrhythmia (Kihara and Morgan, 1991; Haigney et al., 1992; Yeh et al., 2008; Tang et al., 2012). On the other hand, increases in I_{NaL} can effectively lengthen the APD, resulting in EADs (Undrovinas et al., 1999). The authors of previous studies found that inhibiting I_{NaL} significantly prevented arrhythmias such as ventricular tachycardia and ventricular fibrillation (Pezhouman et al., 2014; Markandeya et al., 2016). Therefore, I_{NaL} is considered a new target for the treatment of arrhythmias (Undrovinas and Maltsev, 2008). In the present study, icariin reversed the increases in I_{NaL} induced by ATX-II (a known I_{NaL} opener), decreased I_{CaL}, shortened the APD, and suppressed the EADs induced by ATX-II in LVMs. The percentage inhibitions by 1, 10, 20, and 40 μM icariin of ATX-II augmented I_{NaL} were 7.8 ± 1%, 29 ± 6.4%, 43.68 ± 5.6%, and 61.4 ± 5.7%. The percentage inhibitions by 3, 6, and 9 μM ranolazine of ATX II augmented I_{NaL} were 24 ± 6%, 44 ± 8%, and 62 ± 4% (Luo et al., 2013). The inhibitory effects of icariin on ATX-II augmented I_{NaL} is weaker than ranolazine (a known I_{NaL} blocker). Icariin can inhibit I_{CaL} and shorten APD, thus we concluded that icariin might inhibit ATX-II-induced arrhythmias by blocking I_{NaL} and I_{CaL}.

I_{CaL} is one of the major inward currents in phase 2 of the AP and regulates Ca^{2+}-related physiological processes (Benitah et al., 2010). Extracellular Ca^{2+} flows into cardiomyocytes mainly through L-type calcium channels and subsequently causes elevations in $[Ca^{2+}]_i$,which causes the sarcoplasmic reticulum to release large amounts of Ca^{2+} into the cytosol, a phenomenon known as Ca^{2+}-induced Ca^{2+} release, which increases $[Ca^{2+}]_i$ further. A large number of studies have shown that various pathological conditions, including ischemia/reperfusion injury(de Diego et al., 2008) and heart failure (Casini et al., 2009), are associated with $[Ca^{2+}]_i$ abnormalities, especially intracellular Ca^{2+} overload, which plays a crucial role in the genesis of arrhythmias such as ventricular and atrial fibrillation (Kihara and Morgan, 1991; Yeh et al., 2008). Therefore, inhibiting I_{CaL} can facilitate $[Ca^{2+}]_i$reductions that suppress arrhythmias in the above pathological conditions. In this study, icariin decreased the amplitude of I_{CaL}, which caused a decrease in Ca^{2+} influx. Therefore, icariin exerts class IV antiarrhythmic drug effects by inhibiting I_{CaL}. DADs and TAs can be induced by $[Ca^{2+}]_i$ overload caused by the application of ISO and high $[Ca^{2+}]_o$ (Shutt et al., 2006; Sicouri et al., 2013). In the present study, icariin significantly suppressed DADs and TAs in LVMs, possibly by inhibiting I_{CaL}. Moreover, the inhibition of I_{CaL} induced by icariin in LVMs was 2.8-fold stronger than that induced by icariin in LAMs. Thus, icariin shows a degree of ventricular selectivity with respect to its inhibitory effects on I_{CaL}.

Elevations in $[Ca^{2+}]_i$ increase I_{NaL} by activating the CAMK II and PKC pathways (Ma et al., 2012; Wu et al., 2015). The increased I_{NaL} elevates $[Na^+]_i$, which increases $[Ca^{2+}]_i$ by activating a reverse NCX (Kihara and Morgan, 1991; Haigney et al., 1992; Yeh et al., 2008; Tang et al., 2012). The cellular response may cause or aggravate arrhythmias. In the present study, icariin inhibited both sodium currents (I_{NaT} and I_{NaL}) and I_{CaL}, which blocked the cellular response more effectively, indicating that icariin may be a more effective antiarrhythmic drug than established medications.

I_{Kr} is an important outward current in AP repolarization. Decreases in I_{Kr} lengthen the APD and lead to QT interval prolongation. A variety of noncardiovascular drugs can block I_{Kr}, thereby inducing long QT syndrome and torsade de pointes (TdPs) (Viskin et al., 2003). For example, grepafloxacin, a quinolone antibiotic, was withdrawn from the American drug market because it blocked I_{Kr} significantly and caused excessive QT interval prolongation, resulting in TdPs (Anderson et al., 2001). Therefore, the authors of another study measured I_{Kr} antagonist potency to evaluate the proarrhythmic effects of new drugs (Kim et al., 2016) and found that it did not affect I_{Kr}. In this study, icariin showed no effect on I_{Kr}. Thus, we deemed the compound a safer drug than its established counterparts.

Aconitine, a specific sodium channel agonist, sustained activation of the sodium channels and induced intracellular Na^+ accumulation leading to intracellular Ca^{2+} overload through NCX (Peper and Trautwein, 1967). Moreover, icariin can augment I_{CaL} directly causing intracellular Ca^{2+} overload, which may eventually result in arrhythmias (Zhou et al., 2013). In the present study, we found that icariin increased the onset time and onset dosage of aconitine-induced VPC, VT and VF in whole rabbits. It also decreased the incidence of aconitine-induced VT and VF, as well as mortality in rabbits. The above results indicate that icariin shows cardioprotective effects against aconitine-induced arrhythmias. The cardioprotective effects may be due to reduction of I_{NaT}, I_{NaL} and I_{CaL}.

CONCLUSION

In summary, we found for the first time that icariin exerted class I and IV antiarrhythmic agent effects and moderately inhibited I_{NaL}. Icariin inhibits aconitine-induced arrhythmias in whole rabbits. Icariin also suppressed EADs or DADs and TAs induced by ATX-II or ISO and high $[Ca^{2+}]_o$, respectively, by inhibiting I_{NaT}, I_{NaL}, and I_{CaL}, but had no effect on I_{K1}, I_{Kr}, I_{to}, and I_{Kur}, especially I_{Kr}, which may indicate that icariin is a safer drug than its counterparts. Thus, icariin may have promise as an agent used in the clinical treatment of arrhythmia.

AUTHOR CONTRIBUTIONS

JM designed the research. WJ, MZ, and ZC performed the experiments. ZL, JH, PPZ, YT and PHZ analysis the data. WJ wrote the main text and prepared all of the figures. All authors reviewed and approved this manuscript.

ACKNOWLEDGMENTS

We thank American Journal Experts (AJE) for editing the English of this manuscript.

REFERENCES

Anderson, M. E., Mazur, A., Yang, T., and Roden, D. M. (2001). Potassium current antagonist properties and proarrhythmic consequences of quinolone antibiotics. *J. Pharmacol. Exp. Ther.* 296, 806–810.

Baba, S., Dun, W., Cabo, C., and Boyden, P. A. (2005). Remodeling in cells from different regions of the reentrant circuit during ventricular tachycardia. *Circulation* 112, 2386–2396. doi: 10.1161/CIRCULATIONAHA.105.534784

Benitah, J. P., Alvarez, J. L., and Gomez, A. M. (2010). L-type Ca^{2+} current in ventricular cardiomyocytes. *J. Mol. Cell. Cardiol.* 48, 26–36. doi: 10.1016/j.yjmcc.2009.07.026

Bosch, R. F., Gaspo, R., Busch, A. E., Lang, H. J., Li, G. R., and Nattel, S. (1998). Effects of the chromanol 293B, a selective blocker of the slow, component of the delayed rectifier K^+ current, on repolarization in human and guinea pig ventricular myocytes. *Cardiovasc. Res.* 38, 441–450. doi: 10.1016/S0008-6363(98)00021-2

Casini, S., Verkerk, A. O., van Borren, M. M., van Ginneken, A. C., Veldkamp, M. W., de Bakker, J. M., et al. (2009). Intracellular calcium modulation of voltage-gated sodium channels in ventricular myocytes. *Cardiovasc. Res.* 81, 72–81. doi: 10.1093/cvr/cvn274

Coronel, R., Wilms-Schopman, F. J., Opthof, T., and Janse, M. J. (2009). Dispersion of repolarization and arrhythmogenesis. *Heart Rhythm* 6, 537–543. doi: 10.1016/j.hrthm.2009.01.013

de Diego, C., Pai, R. K., Chen, F., Xie, L. H., De Leeuw, J., Weiss, J. N., et al. (2008). Electrophysiological consequences of acute regional ischemia/reperfusion in neonatal rat ventricular myocyte monolayers. *Circulation* 118, 2330–2337. doi: 10.1161/CIRCULATIONAHA.108.789149

Goldin, A. L. (2002). Evolution of voltage-gated Na^+ channels. *J. Exp. Biol.* 205, 575–584. doi: 10.1242/jeb.110270

Guo, D., Yu, M., Liu, Q., Cox, R. H., Liu, T., and Yan, G. X. (2014). Ventricular hypertrophy amplifies transmural dispersion of repolarization by preferentially increasing the late sodium current in endocardium. *J. Electrocardiol.* 47, 642–648. doi: 10.1016/j.jelectrocard.2014.04.004

Haigney, M. C., Miyata, H., Lakatta, E. G., Stern, M. D., and Silverman, H. S. (1992). Dependence of hypoxic cellular calcium loading on Na^+-Ca^{2+} exchange. *Circ. Res.* 71, 547–557. doi: 10.1161/01.RES.71.3.547

Huang, Z. S., Xiao, H. J., Qi, T., Hu, Z. M., Li, H., Chen, D. L., et al. (2014). Antioxidative protective effect of icariin on the $FeSO_4/H_2O_2$-damaged human sperm based on confocal raman micro-spectroscopy. *J. Huazhong Univ. Sci. Technol. Med. Sci.* 34, 755–760. doi: 10.1007/s11596-014-1348-3

Ke, Z., Liu, J., Xu, P., Gao, A., Wang, L., and Ji, L. (2015). The cardioprotective effect of icariin on ischemia-reperfusion injury in isolated rat heart: potential Involvement of the PI3K-Akt signaling pathway. *Cardiovasc. Ther.* 33, 134–140. doi: 10.1111/1755-5922.12121

Kihara, Y., and Morgan, J. P. (1991). Intracellular calcium and ventricular fibrillation. Studies in the aequorin-loaded isovolumic ferret heart. *Circ. Res.* 68, 1378–1389. doi: 10.1161/01.RES.68.5.1378

Kim, J. G., Sung, D. J., Kim, H. J., Park, S. W., Won, K. J., Kim, B., et al. (2016). Impaired inactivation of L-Type Ca^{2+} current as a potential mechanism for variable arrhythmogenic liability of HERG K^+ channel blocking drugs. *PLoS ONE* 11:e0149198. doi: 10.1371/journal.pone.0149198

Kiyosue, T., and Arita, M. (1989). Late sodium current and its contribution to action potential configuration in guinea pig ventricular myocytes. *Circ. Res.* 64, 389–397. doi: 10.1161/01.RES.64.2.389

Liu, B., Zhang, H., Xu, C., Yang, G., Tao, J., Huang, J., et al. (2011). Neuroprotective effects of icariin on corticosterone-induced apoptosis in primary cultured rat hippocampal neurons. *Brain Res.* 1375, 59–67. doi: 10.1016/j.brainres.2010.12.053

Liu, Z. Q., Luo, X. Y., Sun, Y. X., Wu, W., Liu, C. M., and Liu, S. Y. (2004). The antioxidative effect of icariin in human erythrocytes against free-radical-induced haemolysis. *J. Pharm. Pharmacol.* 56, 1557–1562. doi: 10.1211/0022357044869

Luo, A., Ma, J., Song, Y., Qian, C., Wu, Y., Zhang, P., et al. (2013). Larger late sodium current density as well as greater sensitivities to ATX II and ranolazine in rabbit left atrial than left ventricular myocytes. *Am. J. Physiol. Heart Circ. Physiol.* 306, H455–H461. doi: 10.1152/ajpheart.00727.2013

Ma, J., Luo, A., Wu, L., Wan, W., Zhang, P., Ren, Z., et al. (2012). Calmodulin kinase II and protein kinase C mediate the effect of increased intracellular calcium to augment late sodium current in rabbit ventricular myocytes. *Am. J. Physiol. Cell Physiol.* 302, C1141–C1151. doi: 10.1152/ajpcell.00374.2011

Maoz, A., Christini, D. J., and Krogh-Madsen, T. (2014). Dependence of phase-2 reentry and repolarization dispersion on epicardial and transmural ionic heterogeneity: a simulation study. *Europace* 16, 458–465. doi: 10.1093/europace/eut379

Markandeya, Y. S., Tsubouchi, T., Hacker, T. A., Wolff, M. R., Belardinelli, L., and Balijepalli, R. C. (2016). Inhibition of late sodium current attenuates ionic arrhythmia mechanism in ventricular myocytes expressing LaminA-N195K mutation. *Heart Rhythm* 13, 2228–2236. doi: 10.1016/j.hrthm.2016.08.007

Osadchii, O. E. (2013). Quinidine elicits proarrhythmic changes in ventricular repolarization and refractoriness in guinea-pig. *Can. J. Physiol. Pharmacol.* 91, 306–315. doi: 10.1139/cjpp-2012-0379

Peper, K., and Trautwein, W. (1967). The effect of aconitine on the membrane current in cardiac muscle. *Pflugers Arch. Gesamte Physiol. Menschen Tiere* 296, 328–336. doi: 10.1007/BF00362532

Pezhouman, A., Madahian, S., Stepanyan, H., Ghukasyan, H., Qu, Z., Belardinelli, L., et al. (2014). Selective inhibition of late sodium current suppresses ventricular tachycardia and fibrillation in intact rat hearts. *Heart Rhythm* 11, 492–501. doi: 10.1016/j.hrthm.2013.11.026

Saint, D. A. (2006). The role of the persistent Na^+ current during cardiac ischemia and hypoxia. *J. Cardiovasc. Electrophysiol.* 17(Suppl. 1), S96–S103. doi: 10.1111/j.1540-8167.2006.00390.x

Shutt, R. H., Ferrier, G. R., and Howlett, S. E. (2006). Increases in diastolic $[Ca^{2+}]$ can contribute to positive inotropy in guinea pig ventricular myocytes in the absence of changes in amplitudes of Ca^{2+} transients. *Am. J. Physiol. Heart Circ. Physiol.* 291, H1623–H1634. doi: 10.1152/ajpheart.01245.2005

Sicouri, S., Belardinelli, L., and Antzelevitch, C. (2013). Antiarrhythmic effects of the highly selective late sodium channel current blocker GS-458967. *Heart Rhythm* 10, 1036–1043. doi: 10.1016/j.hrthm.2013.03.023

Song, Y. H., Cai, H., Gu, N., Qian, C. F., Cao, S. P., and Zhao, Z. M. (2011). Icariin attenuates cardiac remodelling through down-regulating myocardial apoptosis and matrix metalloproteinase activity in rats with congestive heart failure. *J. Pharm. Pharmacol.* 63, 541–549. doi: 10.1111/j.2042-7158.2010.01241.x

Sun, X., Jin, X., Zhang, X., Liu, C., Lei, L., Jin, L., et al. (2011). Icariin induces mouse embryonic stem cell differentiation into beating functional cardiomyocytes. *Mol. Cell. Biochem.* 349, 117–123. doi: 10.1007/s11010-010-0666-4

Tan, H. L., Chan, K. G., Pusparajah, P., Saokaew, S., Duangjai, A., Lee, L. H., et al. (2016). Anti-cancer properties of the naturally occurring aphrodisiacs: icariin and its derivatives. *Front. Pharmacol.* 7:191. doi: 10.3389/fphar.2016.00191

Tang, Q., Ma, J., Zhang, P., Wan, W., Kong, L., and Wu, L. (2012). Persistent sodium current and Na^+/H^+ exchange contributes to the augmentation of the reverse Na^+/Ca^{2+} exchange during hypoxia or acute ischemia in ventricular myocytes. *Pflugers Arch.* 463, 513–522. doi: 10.1007/s00424-011-1070-y

Tao, F. F., Qian, C., Guo, W. J., Luo, Q., Xu, Q., and Sun, Y. (2013). Inhibition of Th1/Th17 responses via suppression of STAT1 and STAT3 activation contributes to the amelioration of murine experimental colitis by a natural flavonoid glucoside icariin. *Biochem. Pharmacol.* 85, 798–807. doi: 10.1016/j.bcp.2012.12.002

Undrovinas, A. I., Maltsev, V. A., and Sabbah, H. N. (1999). Repolarization abnormalities in cardiomyocytes of dogs with chronic heart failure: role of sustained inward current. *Cell. Mol. Life Sci.* 55, 494–505. doi: 10.1007/s000180050306

Undrovinas, A., and Maltsev, V. A. (2008). Late sodium current is a new therapeutic target to improve contractility and rhythm in failing heart. *Cardiovasc. Hematol. Agents Med. Chem.* 6, 348–359. doi: 10.2174/187152508785909447

Valdivia, C. R., Chu, W. W., Pu, J., Foell, J. D., Haworth, R. A., Wolff, M. R., et al. (2005). Increased late sodium current in myocytes from a canine heart failure model and from failing human heart. *J. Mol. Cell. Cardiol.* 38, 475–483. doi: 10.1016/j.yjmcc.2004.12.012

Virag, L., Acsai, K., Hala, O., Zaza, A., Bitay, M., Bogats, G., et al. (2009). Self-augmentation of the lengthening of repolarization is related to the shape of the cardiac action potential: implications for reverse rate dependency. *Br. J. Pharmacol.* 156, 1076–1084. doi: 10.1111/j.1476-5381.2009.00116.x

Viskin, S., Justo, D., Halkin, A., and Zeltser, D. (2003). Long QT syndrome caused by noncardiac drugs. *Prog. Cardiovasc. Dis.* 45, 415–427. doi: 10.1016/S0033-0620(03)80005-1

Wang, Q., Hao, J., Pu, J., Zhao, L., Lu, Z., Hu, J., et al. (2011). Icariin induces apoptosis in mouse MLTC-10 Leydig tumor cells through activation of the mitochondrial pathway and down-regulation of the expression of piwil4. *Int. J. Oncol.* 39, 973–980. doi: 10.3892/ijo.2011.1086

Wu, L. (2005). An increase in late sodium current potentiates the proarrhythmic activities of low-risk QT-prolonging drugs in female rabbit hearts. *J. Pharmacol. Exp. Ther.* 316, 718–726. doi: 10.1124/jpet.105.094862

Wu, Y., Wang, L., Ma, J., Song, Y., Zhang, P., Luo, A., et al. (2015). Protein kinase C and Ca^{2+} -calmodulin-dependent protein kinase II mediate the enlarged reverse INCX induced by ouabain-increased late sodium current in rabbit ventricular myocytes. *Exp. Physiol.* 100, 399–409. doi: 10.1113/expphysiol.2014.083972

Xu, C. Q., Liu, B. J., Wu, J. F., Xu, Y. C., Duan, X. H., Cao, Y. X., et al. (2010). Icariin attenuates LPS-induced acute inflammatory responses: involvement of PI3K/Akt and NF-*kappa*B signaling pathway. *Eur J Pharmacol* 642, 146–153. doi: 10.1016/j.ejphar.2010.05.012

Yeh, Y. H., Wakili, R., Qi, X. Y., Chartier, D., Boknik, P., Kaab, S., et al. (2008). Calcium-handling abnormalities underlying atrial arrhythmogenesis and contractile dysfunction in dogs with congestive heart failure. *Circ. Arrhythm. Electrophysiol.* 1, 93–102. doi: 10.1161/CIRCEP.107.754788

Zhang, Q., Li, H., Wang, S., Liu, M., Feng, Y., and Wang, X. (2013). Icariin protects rat cardiac H9c2 cells from apoptosis by inhibiting endoplasmic reticulum stress. *Int. J. Mol. Sci.* 14, 17845–17860. doi: 10.3390/ijms140917845

Zhou, H., Yuan, Y., Liu, Y., Deng, W., Zong, J., Bian, Z. Y., et al. (2014). Icariin attenuates angiotensin II-induced hypertrophy and apoptosis in H9c2 cardiomyocytes by inhibiting reactive oxygen species-dependent JNK and p38 pathways. *Exp. Ther. Med.* 7, 1116–1122. doi: 10.3892/etm.2014.1598

Zhou, Y.-H., Piao, X.-M., Liu, X., Liang, H.-H., Wang, L.-M., Xiong, X.-H., et al. (2013). Arrhythmogenesis Toxicity of Aconitine Is Related to Intracellular Ca^{2+} Signals. *Int. J. Med. Sci.* 10, 1242–1249. doi: 10.7150/ijms.6541

Conflict of Interest Statement: The authors declare that the research was conducted in the absence of any commercial or financial relationships that could be construed as a potential conflict of interest.